Parametric patterns in optical fiber ring nonlinear resonators

K. Staliunas,[1] Chao Hang,[2,3] and V. V. Konotop[2,4]

[1]*ICREA, Departament de Fisica i Enginyeria Nuclear, Universitat Politècnica de Catalunya, Colom 11, E-08222 Terrassa, Barcelona, Spain*

[2]*Centro de Física Teórica e Computacional, Faculdade de Ciências, Universidade de Lisboa, Instituto para Investigação Interdisciplinar, Avenida Professor Gama Pinto 2, Lisboa 1649-003, Portugal*

[3]*State Key Laboratory of Precision Spectroscopy and Department of Physics, East China Normal University, Shanghai 200062, China*

[4]*Departamento de Física, Faculdade de Ciências, Universidade de Lisboa, Campo Grande, Ed. C8, Piso 6, Lisboa 1749-016, Portugal*

(Received 1 June 2013; published 26 August 2013)

We propose that parametrically excited patterns, also known as Faraday patterns, can be observed in nonlinear fiber resonators, where the coefficient of Kerr nonlinearity is periodically varying along the fiber in the resonators. We study the parametric instability analytically on the basis of the Floquet theory and also numerically by direct integration of the system. Instead of a classical Faraday wave excitation scenario, where modulation in time causes the formation of patterns in space, here we propose an inverted scenario, where the modulation in space excites the patterns in time.

DOI: 10.1103/PhysRevA.88.023846 PACS number(s): 42.65.Sf, 42.60.Mi, 05.45.−a, 05.65.+b

I. INTRODUCTION

Parametrically excited patterns, or equivalently Faraday patterns in spatially extended nonlinear systems, can emerge when a parameter of the system is periodically modulated in time, e.g., with the frequency $2\omega_0$. Then the waves (the spatial modes or spatial harmonics) with wave numbers centered at around the critical wave number k_0 can be excited, such that their oscillation frequencies are equal to half of the frequency of the parametric excitation, i.e., with ω_0, related to k_0 via the dispersion relation of the nonlinear media $\omega(k)$. Such patterns were initially observed by Faraday on the surface of a periodically shaken (in a vertical direction) mercury layer [1], where, formally, the magnitude of the gravitation force was periodically modulated in time. The Faraday-like patterns were subsequently observed in vertically shaken granular media [2], in periodically driven spatially extended chemical systems [3,4], and in spatially extended nonlinear optical systems [5]. Not only were the extended Faraday patterns observed [6] but also the localized structures in mechanical [7], chemical [8], and optical [9] systems. More recently the excitation of Faraday patterns of matter waves in repulsive (defocusing-type) Bose-Einstein condensates (BECs) subjected to temporal periodic modulation of the nonlinearity coefficient (the atomic scattering length) was predicted theoretically [10,11] and observed experimentally [12].

A parametric pattern formation, in principle, is possible in nonlinear optics for the light waves (either spatial beams or temporal pulses) propagating along the matter with the Kerr nonlinearity modulated *in space* in a longitudinal (along the propagation) direction. Like in Refs. [1–12], the modulation-ally stable case is considered; i.e., the sign of nonlinearity is such that no filamentation in two-dimensional (2D) beams and no soliton formation from 1D pulses are possible. If the nonlinearity coefficient of the media is modulated along the propagation direction with the spatial wave number $2q$, then, simply speaking, the "flying" photon experiences a temporal modulation of nonlinearity along the propagation coordinate with the corresponding frequency $2\omega_0 = c2q$. This sets the analogy with the parametric pattern excitation by modulating the system in time, as in previous references [1–12]. The process then leads to the transverse modulation of the light beams by $k_\perp$ (for transversally extended systems) or to longitudinal modulation of light pulses by $k_{||}$ (in optical fibers). The selection of $k_\perp$ or $k_{||}$ is determined by the diffraction or dispersion relations of the matter depending on the geometry (whether we consider monochromatic beams or wave pulses). The mathematical description of the Faraday instability in the above-presented cases in optics is identical to the Faraday instability in BECs [10,11], as the paraxial wave propagation equation for beams or the wave envelope equation for pulses is analogous to the Gross-Pitaevskii equation.

The parametric instability of the pulses propagating along the nonlinear fibers has been studied in Ref. [13], where a periodically modulated Kerr nonlinearity in a normal dispersion regime was considered. A parametric excitation of transverse modulation (transverse Faraday instability) in nonlinear optics has never been considered for propagating waves to the best of our knowledge, although its mathematical description should be analogous to the longitudinal Faraday effect analyzed in Ref. [13]. In the present work we describe how one can realize very naturally the parametric Faraday instability in optical systems by using Kerr nonlinear fiber *resonators*.

Let us assume, that in a fiber resonator, as illustrated in Fig. 1, the nonlinearity coefficient along the resonator is modulated with the spatial period equal to half of the resonator length; i.e., the nonlinearity makes two modulation periods during the roundtrip. In this case the longitudinal parametric instability of the light pulses could be supported by the resonator, as the period of the emerging modulation being half the period of the nonlinearity modulation would perfectly fit the length of the resonator, i.e., would be supported by the resonator condition.

Before starting the mathematical description, we inspect the proposed system in terms of the fiber resonator modes. Let the mode $k_m = 2\pi m/L$, which has the frequency ω_m following from the dispersion relation of fiber is excited by the external injection, i.e., by the external wave with the frequency ω_{inj} close to ω_m. The modulation of nonlinearity along the resonator excites the quasimodes with $m + 2$ and

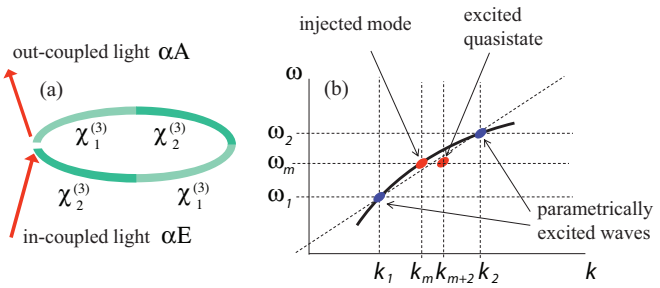

FIG. 1. (Color online) (a) Fiber resonator with the nonlinearity coefficient varying periodically (making two periods) along the resonator length. (b) The longitudinal mode structure and the dispersion relation of the resonator. (The curvature of the dispersion curve is exaggerated.) The injected mode (k_m,ω_m) and the excited nonresonant quasistate (k_{m+2},ω_m) are shown by red ellipses (on the horizontal dashed line at ω_m); the parametrically excited modes at (k_1,ω_1) and (k_2,ω_2) are shown by blue ellipses (on the horizontal dashed lines at ω_1 and ω_2).

$m-2$ indices. The parametric excitation process is as follows: two excitations, one from the ground-state mode (k_m,ω_m) and the other from the nonresonant quasistate (k_{m+2},ω_m), get mixed and annihilate, and two new resonant excitations appear at (k_1,ω_1) and (k_2,ω_2), obeying the energy and momentum conservation relations: $\omega_1+\omega_2=2\omega_m$ and $k_1+k_2=k_m+k_{m+2}$.

The described mechanism is illustrated in Fig. 1(b), where the dispersion is deliberately exaggerated. As it is typical for fiber resonators, the curvature of the dispersion curve is very small; consequently very remote modes enter into the resonance and are parametrically excited. The resonance conditions can be estimated considering the series expansion of the material dispersion $k(\omega)=k_m+\beta_1(\omega-\omega_m)+\beta_2(\omega-\omega_m)^2/2+\cdots$. The frequencies of the parametrically excited modes more conveniently can be written in the form $\omega_{1,2}=\omega_m\pm\omega_0$, where the parametrically excited sideband frequency obeys $\omega_0=\sqrt{2q/\beta_2}$. For a fiber loop of one meter length ($L=1$ m), for the wavelength of the order $\lambda=10^{-6}$ μm, and for the typical dispersion of the waveguide $\beta_2\approx 20$ ps^2/km, the sideband frequency is $\omega_0\approx 2.2\times 10^{13}$ s^{-1}, i.e., 4 orders of magnitude larger than the mode frequency separation for the same resonator: $\Delta\omega\approx 3\times 10^9$ s^{-1}.

A closer inspection of the mode representation in Fig. 1 suggests a generalization to an arbitrary number of periods of nonlinearity along the resonator. This technically can be realized from $2p$ pieces of fibers with two different nonlinear coefficients, joined in alternating order. Therefore in the following, in analytic study we consider the general case of p-period modulation along the resonator loop.

II. THE MODEL

We consider the light propagation along the fiber by solving the nonlinear Schrödinger equation (NLSE) for the field envelope $A^{(n)}(\tau,z)$,

$$\partial A^{(n)}(\tau,z)/\partial z=-i\partial^2 A^{(n)}(\tau,z)/\partial\tau^2+ic(z)|A^{(n)}(\tau,z)|^2A^{(n)}(\tau,z),\qquad(1a)$$

defined for each (the nth) resonator roundtrip; τ varies between 0 and T, where T is the period of a roundtrip. The reference frame moves with the group velocity of light; therefore the first time derivatives of the field envelopes do not appear in Eq. (1a). The retarded time τ is scaled to make the second-order dispersion coefficient unity. The nonlinearity coefficient is considered periodic, with the period $L/(2p)$, where p is an integer and L is the length of the resonator. The modulation wave number is then $2q=4\pi p/L$. In numerical calculations we consider harmonic modulation of the coefficient of nonlinearity $c(z)=c_0+2\Delta c\cos(2qz)$; however the basic results hold for arbitrary (e.g., a steplike) functions of nonlinearity. It is important that the average nonlinearity c_0 is positive. We also take care that the nonlinearity remains positive during the entire roundtrip: $2\Delta c<c_0$ in order to exclude any possibility that the system enters into a modulationally unstable regime during a single roundtrip (i.e., the system remains all the time in the modulationally stable regime).

Equation (1a) must be completed by the condition relating the fields at the end ($z=L$) of the current (nth) resonator roundtrip and at the beginning ($z=0$) of the next ($n+1$) roundtrip:

$$A^{(n+1)}(\tau,0)=(1-\alpha)A^{(n)}(\tau,L)e^{i\varphi}+\alpha E(\tau),\qquad(1b)$$

which means that (i) an external field is injected with the envelope $E(\tau)$, which is either a continuous wave, $E(\tau)=\text{const}=E_0$, or a pulse from the pulse train of the period synchronized with the length of the resonator; (ii) a fraction α of the field is decoupled from the fiber resonator; and (iii) the propagation along the fiber results in some linear phase shift φ with respect to the external injection, which is either due to a particular reference frame of NLSE (1a) or due to an out-coupling mechanism introducing a particular phase shift.

The system (1) is a well-known Ikeda map [14,15] widely used to simulate light propagation in fiber lasers and resonators. In particular Eqs. (1a) and (1b) were used in Refs. [16,17] to study the stability of the Kerr resonator without any spatial modulation of nonlinearity. We note however, that the system (1) does not require the continuity and differentiability of the field at the ends of the resonator; i.e., generally speaking $A^{(n+1)}(\tau,0)\neq A^{(n)}(\tau,L)$ (unless a specific form of the solution is chosen, see Eq. (2) below, or the pulsed injection case is considered). Moreover, it has been shown in Ref. [18] that the continuity condition can eliminate some instabilities of the system; i.e. in other words some instabilities observed in Refs. [16,17] can occur due to the abovementioned discontinuity. In this context we also mention that alternatively to the Ikeda map (1), which is integrated throughout the present paper, continuous-wave models are being developed [18,19] where the field persists continuously when passing through the cavity input (output). The parametric instability can be also demonstrated in continuous-wave models as our preliminary results indicate; here, however, we restrict our analysis to using a more simple Ikeda model (1).

III. STABILITY ANALYSIS

A. Homogeneous solution of the map

We start with the linear stability analysis of a homogeneous solution; i.e., we assume that the injection is a continuous

wave: $E(\tau) = \text{const} = E_0$. The respective solution of Eq. (1a) reads

$$A^{(n)}(z) = A_0^{(n)} e^{i|A_0^{(n)}|^2 \int c(z)dz}. \tag{2}$$

At the end of each resonator roundtrip $A^{(n)}(L) = A_0^{(n)} e^{i|A_0^{(n)}|^2 c_0 L} = A_0^{(n)} e^{i\theta}$, where $A_0^{(n)}(0) = A_0$ is a constant field and $\theta = |A_0^{(n)}|^2 c_0 L$ is a nonlinear phase shift accumulated during propagation along the fiber. The resonator end-roundtrip condition (1b) in the stationary case allows us to calculate the amplitude of the field as the solution of the transcendental equation

$$A_0 = (1-\alpha) A_0 e^{i\varphi + i\theta} + \alpha E_0. \tag{3}$$

B. Linear stability analysis

Next we perform linear stability analysis of the map (1) with respect to the sideband modes. We consider in a standard way the exponential oscillatory growth of a small harmonic mode of perturbation:

$$A^{(n)}(z,\tau) = A_0^{(n)}(z)[1 + a^{(n)}(z)\cos(\omega\tau)], \tag{4}$$

where $\omega = \frac{2\pi}{T}$. The resonator end-roundtrip condition also applies to the perturbation

$$a^{(n+1)}(0) = (1-\alpha) a^{(n)}(L) e^{i(\phi+\theta)}, \tag{5}$$

as it follows from Eqs. (1b) and (3). We also notice that the ansatz (4) implies that

$$A^{(n)}(z,0) = A^{(n)}(z, 2\pi/\omega), \tag{6}$$

which can be viewed as a constraint (boundary conditions on the domain $[0,T]$) additional to Eq. (1b).

A goal of the analysis is the calculation of the Floquet multipliers (the multipliers indicating the growth of perturbation on one full resonator roundtrip) depending on the frequency of the emerging modulation ω. If the modulus of the largest multiplier is larger than 1, then the map is unstable, and the corresponding modulation mode grows.

It is known that even the stability analysis of the NLSE with periodically modulated nonlinearity cannot be performed analytically without simplifications [20,21]. Here we face additionally the effects of the resonator end-roundtrip condition that make the analysis even more complicated. Therefore we follow two alternative approaches: (i) a numerical approach, calculating the evolution of perturbations numerically over the full resonator roundtrip (the propagation along the nonlinear fiber plus the resonator end-roundtrip condition, i.e., losses, phase shift, and the injection) and then calculating the Floquet multipliers numerically by diagonalizing the perturbation evolution matrix; and (ii) a simplified analytic approach, considering a weak modulation of nonlinearity and a weak and harmonic response.

C. Numerical stability analysis

A standard technique is used: we find the homogeneous stationary solution (3), add a small harmonic perturbation, $a^{(n)} = \varepsilon\cos(\omega\tau)$, and calculate the evolution of the perturbation over a full resonator roundtrip integrating numerically Eq. (1). We ensure that the perturbation is sufficiently small (we are still in a linear regime with respect to the perturbation) checking that the modulation at the other harmonics of the excitation do not appear in one roundtrip. The procedure is repeated for a set of two independent perturbations: $a_1^{(n)} = \varepsilon\cos(\omega\tau)$ and $a_2^{(n)} = i\varepsilon\cos(\omega\tau)$. In this way the map is numerically calculated and a 2×2 matrix is obtained, relating the real and imaginary parts of perturbation at the beginning of the nth and $(n+1)$ th resonator roundtrips. The matrix is numerically diagonalized, and the Floquet multipliers are calculated as the eigenvalues of the map. The modulus of the largest eigenvalue indicates the stability of the perturbation.

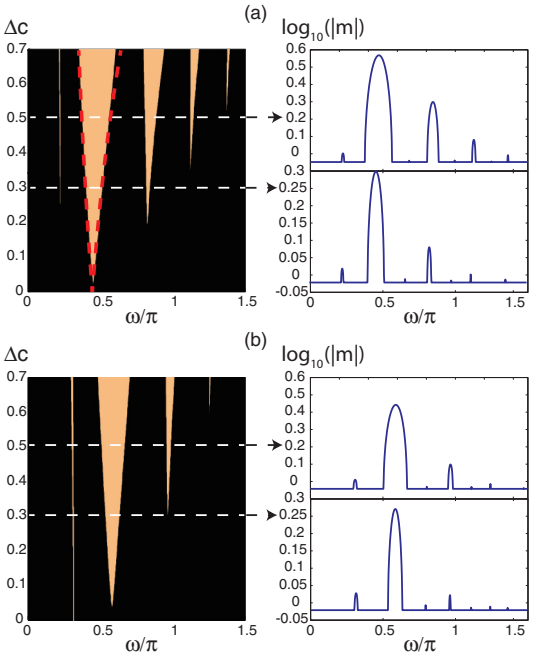

FIG. 2. (Color online) Numerically calculated instability domains [on the plane $(\omega, \Delta c)$] for the near-resonant (a) and far-off-resonant (b) cases. The dashed lines in panel (a) indicate the analytically calculated instability boundary corresponding to first Arnold tongue [see Eq. (10)]. Parameters: $c_0 = 1.0$, $L = 1.0$, $\alpha = 0.1$, $E_0 = 3.3$; also $\varphi = -8.5$ for panel (a) and $\varphi = -4.0$ for panel (b). The insets show the moduli of dominating Floquet multipliers in logarithmic scale ($\log_{10}(|m|)$) for different Δc : $\Delta c = 0.3$ and $\Delta c = 0.5$ (indicated by horizontal lines).

Figure 2 shows the instable areas of the map. In Fig. 2(a) a nearly resonant case is considered, i.e., the situation where the nonlinear phase shift of the homogeneous solution $\theta = |A_0^{(n)}|^2 c_0 L$ is approximately compensated by the linear phase shift $\theta + \varphi \approx 0$. In Fig. 2(b) a strongly nonresonant case is calculated. In both cases the instability areas are visible (the so-called "Arnold tongues") [20,21]. The instability areas, as expected, increase with the amplitude of modulation of nonlinearity. In the close-to-resonance case the instabilities are generally stronger than those in the far-from-resonant case, as the amplitude of the homogeneous solution (and consequently all the nonlinear effects) is higher.

The structure of the Arnold tongues resembles that in a dissipative NLSE, as follows, e.g., from comparison with Ref. [10]. However some differences with the stability diagram of the dissipative NLSE in Ref. [10] are envisaged: Apart from the parametric instability tongues, another instability related due to presence of the resonator appears [see Fig. 2(b)]. This instability typically appears in a far-from-resonant case and is not related to the modulation of nonlinearity. Such instability of fiber ring resonators modeled by Eqs. (1a) and (1b) in the normal dispersion regime has been found and discussed by Haelterman [16] and Coen and Haelterman [17].

Note also that the frequency of the most unstable mode (the tip of the first Arnold tongue) depends on the linear phase shift φ. This is due to the dependence of the amplitude of the stationary state A_0 on the linear phase shift, as follows from the transcendental equation (3).

D. Approximate stability analysis

We split the analysis into two stages: (i) the conservative nonlinear propagation along the fiber governed by modulated NLSE (1a), and (ii) the transformation of fields at the end of the resonator roundtrip (1b).

(i) Assuming, that the modulation is weak, the perturbation of the NLSE solution is searched in the form of expansion into spatial harmonics with the period of multiples of half of the period of modulation of nonlinearity:

$$A^{(n)}(z,\tau) = A_0^{(n)}(z)\{1 + [a_0^{(n)}(z) + a_{+1}^{(n)}(z)e^{iqz} + a_{-1}^{(n)}(z)e^{-iqz} + \cdots]\cos(\omega\tau)\}, \tag{7}$$

where $q = 2\pi p/L$ is half of the modulation wave number, $A_0^{(n)}(z)$ is the solution of the map in stationary regime (3), and $a_j^{(n)}(z)$ are the slowly varying amplitudes of the corresponding harmonics of the perturbation. For the sake of simplicity, below we drop the upper index (i.e., the number of roundtrips) since the consideration is limited to one trip only.

The expansion (7) is plugged into Eq. (1a), and an infinite set of coupled equations for the harmonics of perturbations (in terms of q) is obtained. After diagonalization of the linear system the eigenvalues can be, in principle, calculated and, in this way, the linearized version of NLSE (1a) can be integrated over a $2p$ modulation period (over one resonator roundtrip). This can be done only numerically by truncating the infinite chain of equations. In order to estimate roughly the instability, a substantial simplification is possible by truncation of the expansion to only two harmonics, those with q and $-q$ in expansion (7) (i.e., the use of only harmonic in space perturbation at half of the excitation frequency):

$$da_1/dz = i(\omega^2 - q)a_1 + ic_0|A_0|^2(a_1 + a_{-1}^*) + i\Delta c|A_0|^2(a_{-1} + a_1^*), \tag{8a}$$

$$da_{-1}/dz = i(\omega^2 + q)a_{-1} + ic_0|A_0|^2(a_{-1} + a_1^*) + i\Delta c|A_0|^2(a_1 + a_{-1}^*). \tag{8b}$$

The growth exponents of Eqs. (8a) and (8b) are found by calculating the eigenvalues of the matrix of the coefficients [note that the 4×4 matrix must be diagonalized, due to complex character of Eqs. (8a) and (8b)]: The dominating eigenvalue (the one with the largest increment),

$$\lambda = \sqrt{-q^2 - \omega^2(2c_0|A_0|^2 + \omega^2) + 2\omega\sqrt{(\Delta c|A_0|^2)^2\omega^2 + q^2(2c_0|A_0|^2 + \omega^2)}}, \tag{9}$$

describes the first Arnold tongue of the instability of the NLSE. As only the first harmonics is considered in the expansion (7), only the first Arnold tongue is obtained (a truncation to higher harmonics would reproduce the higher-order instability tongues).

The first Arnold tongue, according to Eq. (7), is centered at the following frequency:

$$\omega_0^2 = -c_0|A_0|^2 + \sqrt{(c_0|A_0|^2)^2 + q^2}. \tag{10}$$

And the instability is bounded by

$$\Delta c|A_0|^2 = \frac{q^2}{2\omega^2} - c_0|A_0|^2 - \frac{\omega^2}{2} \quad \text{for} \quad \omega < \omega_0, \tag{11a}$$

$$\Delta c|A_0|^2 = -\left(\frac{q^2}{2\omega^2} - c_0|A_0|^2 - \frac{\omega^2}{2}\right) \quad \text{for} \quad \omega > \omega_0. \tag{11b}$$

At the resonance frequency $\omega = \omega_0$ and for weak modulation, $\Delta c|A_0|^2 \ll 1$ (i.e., at around the tip of the first Arnold tongue in Fig. 3), Eq. (9) simplifies to

$$\lambda = \frac{\Delta c|A_0|^2}{q} \times \sqrt{2(c_0|A_0|^2)^2 + q^2 - 2c_0|A_0|^2\sqrt{(c_0|A_0|^2)^2 + q^2}}. \tag{12}$$

Generally, the NLSE must be solved for the propagation along the fiber, and the transformation relating the evolution of the perturbations in a roundtrip [e.g., in the basis of $(a_1, a_1^*, a_{-1}, a_{-1}^*)$] must be calculated as a 4×4 matrix $\hat{N}$ (not defined explicitly in the text, due its clumsy form).

(ii) The condition at the end of the roundtrip in the basis of $(a_1, a_1^*, a_{-1}, a_{-1}^*)$ reads [as directly follows from Eq. (5)]

$$\hat{R} = (1 - \alpha)\hat{D}(e^{i(\varphi+\theta)}, e^{-i(\varphi+\theta)}, e^{-i(\varphi+\theta)}, e^{-i(\varphi+\theta)}), \tag{13}$$

where $\hat{D}$ is a diagonal matrix.

The maps describing the evolution of perturbation in nonlinear propagation $\hat{N}$ and at the end of resonator roundtrip

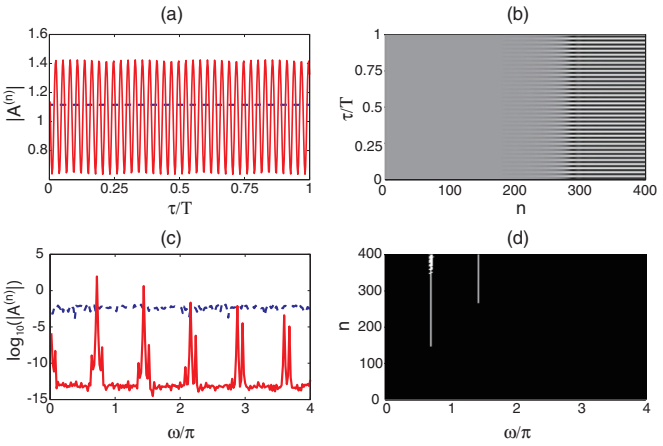

FIG. 3. (Color online) The field dynamics in the case of constant injection $E(\tau) = E_0$. (a) The envelopes (amplitudes) of the field $A^{(n)}$ for $n = 0$ ($|A^{(0)}| = |A_0| = 1.12$; dashed line) and for $n = 400$ (solid line). n is the number of roundtrips. (b) The evolution of the envelopes. (c) The spectra in log scale ($\log_{10}(|A^{(n)}|)$) for $n = 0$ (dashed line) and for $n = 400$ (solid line). (d) The evolution of the spectrum. The first Arnold tongue at $\omega/\pi \approx 0.7$ corresponds well with that estimated from the linear stability analysis. The parameters are $\alpha = 0.1$, $\varphi = -1.1$, $E_0 = 2.0$, $c_0 = 1.0$, $\Delta c = 0.175$, and $L = 1.0$. A small perturbation of amplitude 10^{-3} is added to trigger the instability.

condition $\hat{R}$ must be considered together by calculating the matrix product $\hat{R}\hat{N}$ and diagonalized in order to obtain the Floquet multipliers for the full resonator roundtrip. Again the explicit analytical expression is impossible in the general case, as the stationary values of $|A_0|^2$, and consequently the θ values, are given by the transcendental equation (3). However, restricting to a special case of the resonance $\theta + \varphi = 0$, the resonator end-roundtrip matrix becomes proportional to the unit matrix $\hat{R} = (1 - \alpha)\hat{I}$, and the analysis substantially simplifies. In particular the four Floquet multipliers depend solely on their "own" Lyapunov exponents of the NLSE perturbation (the NLSE perturbation modes do not couple mutually at the end of the resonator roundtrip) and read $m_i = (1 - \alpha)e^{\lambda_i L}$. Then it remains to consider only the dominating instability calculated in Eqs. (9) and (12), and the stability condition becomes $\lambda L + \ln(1 - \alpha) > 0$, which for $\alpha \ll 1$ simplifies to $\lambda L/\alpha > 1$.

As a rough approximation, for the resonant excitation $\omega \approx \omega_0$ the largest growth exponent in conservative propagation is $\lambda \approx \Delta c|A_0|^2$ [here Eq. (12) was simplified in the short wavelength limit $q \gg (c_0|A_0|^2)$]; therefore the instability condition is $L\Delta c|A_0|^2 > \alpha$. This is a good guiding point in the search for the parametric instability in numerics and experiments. The physical interpretation of the latter relation is the following: the parametric instability in the ring Kerr nonlinear cavity develops if the overall variation of the modulus of the nonlinear phase shift is larger than the losses during the roundtrip. In other words, if the Kerr cavity is constructed from the pieces of fibers with nonlinearity coefficients c_1 and c_2, then the characteristic nonlinear phase shift difference $L|\Delta c||A_0|^2 \approx L|c_1 - c_2||A_0|^2/2$ in a roundtrip must be of the order of, or larger than, the roundtrip loss for the development of the parametric instability.

IV. NUMERICAL STUDY OF EVOLUTION

We have performed full numerical simulations of the map (1) by solving consequently the NLSE (1a) for wave propagation along the loop and then applying the resonator end-roundtrip condition (1b). We consider the following two cases: (i) a plane wave $E(\tau) = E_0$ is applied; and (ii) excitation by Gaussian pulses $E(\tau) = E_0 \exp[-(\tau - T/2)^2/\tau_0^2]$.

The first case [the plane wave $E(\tau) = E_0$] gives a numerical demonstration of the above found and analyzed instability. In the numerical calculation, we first calculate the stationary solution from the transcendental equation (3). Then, a small δ-correlated noise (typically of amplitude 10^{-3}) is added to the stationary solution in order to trigger the instability. Finally, we solve the map (1) for 400 roundtrips and represent the field in time and frequency domain. In order to obtain a more regular evolution we stay close to the instability boundary in parameter space: we take a relatively small modulation of nonlinearity, $\Delta c = 0.175$, while keeping the condition $L\Delta c|A_0|^2 > \alpha$ satisfied. The evolution is summarized in Fig. 3. The threshold and frequencies of excited modes of the instability correspond well with those estimated from the linear stability analysis.

For a larger amplitude of modulation of the nonlinearity coefficient the parametrically excited pattern was no more stationary. In particular for $\Delta c = 0.25$, periodic revivals of the emerging patterns were observed, similarly to those reported in Ref. [22] for pure parametrically modulated NLSE. For an even larger amplitude of nonlinearity modulation, e.g., for $\Delta c = 0.35$, a chaotic evolution of the field as initiated by the predicted instability is obtained as shown in Fig. 4.

The second case (the excitation by Gaussian pulse $E(\tau) = E_0 \exp[-(\tau - T/2)^2/\tau_0^2]$, with $\tau_0 = T/6$ in this particular case) shows the persistence of the instability and of the pattern formation. In the numerical calculation, we first solve the map (1) for 100 resonator roundtrips without the modulation of the nonlinearity. After the stationary pulse sets in the resonator (with the envelopes different from the envelope of the Gaussian

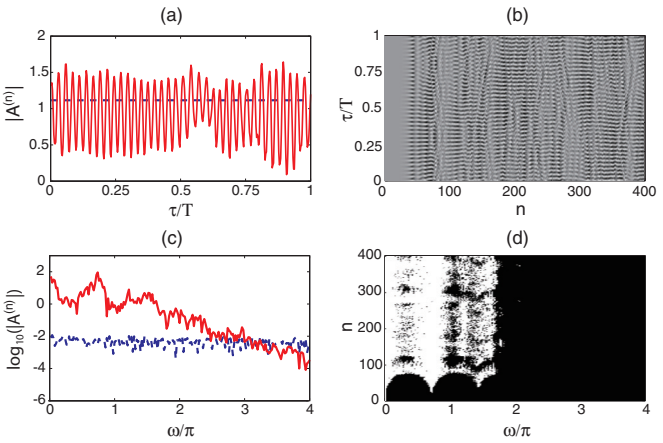

FIG. 4. (Color online) The spatiotemporally chaotic evolution of the field in the case of constant injection $E(\tau) = E_0$. Each panel corresponds to the one with the same label of Fig. 3. The parameters are the same with those given in Fig. 3, except for $\Delta c = 0.35$.

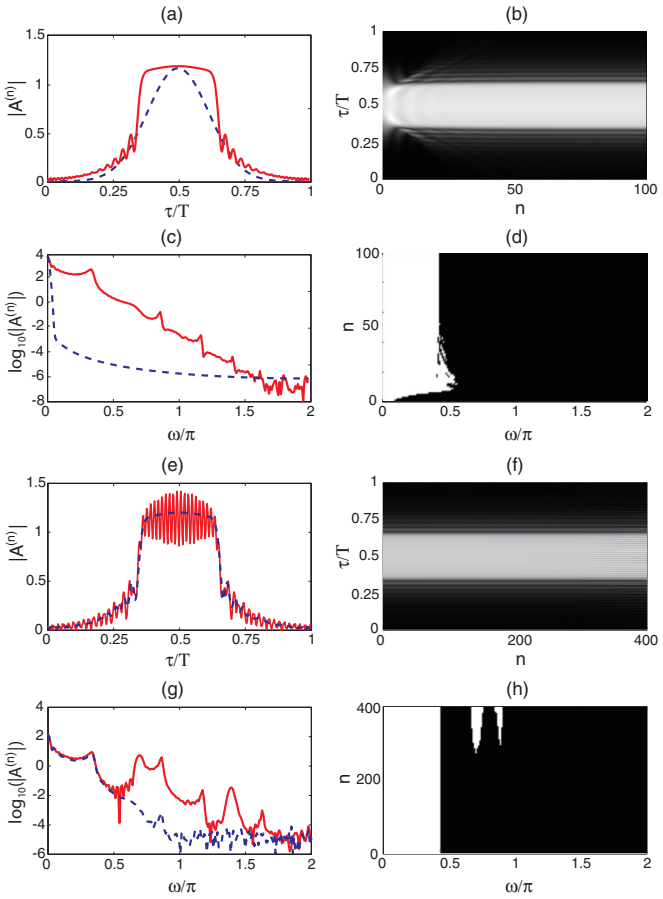

FIG. 5. (Color online) Evolution of the field for injection in the form of Gaussian pulses $E(\tau) = E_0 \exp[-(\tau - T/2)^2/\tau_0^2]$, with $\tau_0 = T/6$. Panels (a)–(d) were obtained with $\Delta c = 0$, while Panels (e)–(h) were obtained with $\Delta c = 0.206$. Panels (a) and (e): The modules of the field $A^{(n)}$ for $n = 0$ (dashed line) and for $n = 100$ and 400 (solid line). Panels (b) and (f): The evolution of the envelope. Panels (c) and (g): The spectra in log scale $[\log_{10}(|A^{(n)}|)]$ for $n = 0$ (dashed line) and for $n = 100$ and 400 (solid line). Panels (d) and (h): The evolution of the spectrum. The first Arnold tongue is still at $\omega/\pi \approx 0.7$ [see panel (h)], which matches well with the estimate obtained from the linear stability analysis. The parameters are $\alpha = 0.1$, $\varphi = -1.2$, $E_0 = 3.0$, $c_0 = 1.0$, and $L = 1.0$.

pulse of injection), the modulation of the nonlinearity is switched on. In the latter case of pulsed injection, the random perturbation is not necessary to trigger the instability, which is different from the previous case of the homogeneous pump. The subsequent iteration for 400 roundtrips of the map (1) with the modulation of the nonlinearity indicates the growth of instable modes, as summarized in Fig. 5. The frequency of the instability in this latter case is in good correspondence with the former case and the analytical estimation.

V. CONCLUSIONS

Summarizing, we predict the parametric instability in a Kerr nonlinear fiber cavity. We discuss the analogy between the Kerr nonlinear fiber resonator with the "conventional" systems showing the Faraday instability. We show the emergence of the patterns by the linear stability analysis (based on the Floquet theory). Finally we prove the pattern formation by solving the nonlinear Ikeda map.

We emphasize that the reported instability has nothing to do with the modulational instability. The latter occurs in fibers *(and fiber resonators)* in the anomalous dispersion case, when also the soliton formation is possible. Here we have the opposite situation. Moreover, the modulation instability is a long-wave instability, and here we observe the well-controllable, short-wave instability, typical of parametrically excited instabilities.

Finally, we note that the character of the Faraday pattern formation process is reversed. In the classical situation the temporal modulation of some parameters (e.g., nonlinearity) excites parametrically the spatial Faraday waves and patterns; here the spatial modulation (along the fiber) of nonlinearity excites the periodic in time modulation of the wave or of the envelope of the pulse.

ACKNOWLEDGMENTS

The work is financially supported by the Spanish Ministerio de Educación y Ciencia and the European FEDER through Project No. FIS2011-29734-C02-01, by the FCT under Grant No. PEst-OE/FIS/UI0618/2011, and by the Acciones Integradas Spain-Portugal PT2009-0089 (Grant No. E-27/10).

[1] M. Faraday, Philos. Trans. R. Soc. London **121**, 319 (1831).
[2] F. Melo, P. B. Umbanhowar, and H. L. Swinney, Phys. Rev. Lett. **72**, 172 (1994) .
[3] V. Petrov, Q. Ouyang, and H. L. Swinney, Nature (London) **388**, 655 (1997).
[4] A. L. Lin, M. Bertram, K. Martinez, H. L. Swinney, A. Ardelea, and G. F. Carey, Phys. Rev. Lett. **84**, 4240 (2000).
[5] K. Staliunas and V. J. Sanchez-Morcillo, *Transverse Patterns in Nonlinear Optical Resonators*, Springer Tracts in Modern Physics, Vol. 183 (Springer, Berlin, 2003).
[6] M. C. Cross and P. C. Hohenberg, Rev. Mod. Phys. **65**, 851 (1993).
[7] S. J. Moon, M. D. Shattuck, C. Bizon, D. I. Goldman, J. B. Swift, and H. L. Swinney, Phys. Rev. E **65**, 011301 (2001).
[8] S. Fauve and O. Thual, Phys. Rev. Lett. **64**, 282 (1990).
[9] V. B. Taranenko, K. Staliunas, and C. O. Weiss, Phys. Rev. Lett. **81**, 2236 (1998).
[10] K. Staliunas, S. Longhi, and G. J. de Valcárcel, Phys. Rev. Lett. **89**, 210406 (2002).
[11] K. Staliunas, S. Longhi, and G. J. de Valcárcel, Phys. Rev. A **70**, 011601 (2004).
[12] P. Engels, C. Atherton, and M. A. Hoefer, Phys. Rev. Lett. **98**, 095301 (2007).
[13] F. Kh. Abdullaev *et al.*, J. Opt. Soc. Am. B **14**, 27 (1997).
[14] K. Ikeda, Opt. Commun. **30**, 257 (1979).
[15] K. Ikeda, H. Daido, and O. Akimoto, Phys. Rev. Lett. **45**, 709 (1980).
[16] M. Haelterman, Opt. Lett. **17**, 792 (1992).

[17] S. Coen and M. Haelterman, Phys. Rev. Lett. **79**, 4139 (1997).
[18] D. A. Zezyulin, V. V. Konotop, and M. Taki, Opt. Lett. **36**, 4623 (2011).
[19] M. Tlidi, A. Mussot, E. Louvergneaux, G. Kozyreff, A. G. Vladimirov, and M. Taki, Opt. Lett. **32**, 662 (2007).
[20] P. Coullet, T. Frisch, and G. Sonnino, Phys. Rev. E **49**, 2087 (1994).
[21] W. Zhang and J. Viñals, Phys. Rev. E **53**, R4283 (1996).
[22] Yu. Kagan and L. A. Maksimov, Phys. Rev. A **64**, 053610 (2001).